Intumescence behaviour of bottom ash based geopolymer mortar through microwave irradiation – As affected by alkali activation

Article *in* Construction and Building Materials · November 2016

DOI: 10.1016/j.conbuildmat.2016.08.135

5 authors, including:

Ehsan Ul Haq
Università del Salento
10 PUBLICATIONS **46** CITATIONS
SEE PROFILE

Sanosh Padmanabhan Kunjalukkal
Università del Salento
43 PUBLICATIONS **522** CITATIONS
SEE PROFILE

Antonio Licciulli
Università del Salento
103 PUBLICATIONS **1,500** CITATIONS
SEE PROFILE

Construction and Building Materials 126 (2016) 951–956

Contents lists available at ScienceDirect

Construction and Building Materials

journal homepage: www.elsevier.com/locate/conbuildmat

Intumescence behaviour of bottom ash based geopolymer mortar through microwave irradiation – As affected by alkali activation

Ehsan Ul Haq [a,*], Sanosh Kunjalukkal Padmanabhan [b], Muhammad Zubair [a], Liaqat Ali [a], Antonio Licciulli [b]

[a] Department of Metallurgical and Materials Engineering (MME), UET Lahore, 54890, Pakistan
[b] Department of Engineering for Innovation, University of Salento, Lecce 73100, Italy

HIGHLIGHTS

- Effect of alkali over foamability of bottom ash geopolymer is studied.
- Optimum alkali activation to tailor various properties.
- Alkali activation produces narrow pore size range, high strength and elastic moduli.
- Higher degree of geopolymerization is achieved in geopolymer foams.
- All claims are justified by characterization and related literature.

ARTICLE INFO

Article history:
Received 18 January 2016
Received in revised form 21 August 2016
Accepted 28 August 2016

Keywords:
Intumescence of mortar
Alkali effect
Microwave
Bottom ash
Geopolymer foam

ABSTRACT

In this research the effect of alkali over the microwave enhanced bottom ash based geopolymer foam, is studied. Various samples using bottom ash and sodium silicate were prepared by varying the amounts of alkali. The higher amounts of alkali were compensated by reducing the sodium silicate percentages in order to keep the relative amounts of bottom ash and other ingredients constant. In the absence of alkali activation, the expansion in the slurry is more compared to alkali activated slurry but the porosity distribution is not so uniform as in the case of alkali activated geopolymer foam. Furthermore, a pipe also appeared in the center of non-alkali treated samples. The porosity was uniform in morphology and distribution from top to bottom for the alkali activated geopolymer foams hence properties as well. The increased amount of sodium hydroxide enhanced the properties till 5% by weight. The strength is found to be more by the use of alkali upto 3.15 MPa with 5% sodium hydroxide solution. The properties developed in the foams are justified by the TGA, DTA, FTIR and SEM analysis. Higher surface area was obtained for the samples without alkali activation compared to alkali activated samples.

1. Introduction

Many construction materials are being considered among the non-sustainable material because ever increasing demand cannot be successfully met without further investigations and discovering new sources as construction materials. The Portland cement is considered also among these because the raw materials for its production and the energy required in processing is so high that in near future both may not be successfully coped [1,2]. Among various other new emerging approaches, geopolymer is prominent in a sense of cost and availability of the raw materials. The term geopolymer first used by Davidovits to introduce the chemical reaction between silica and alumina tetrahedra to form an inorganic polymer by the condensation reaction. In this process first the aluminosilicate source is activated by mixing with highly alkaline solution usually of sodium hydroxide and potassium hydroxide [3,4]. The Fly ash and bottom ash are the industrial wastes left after burning fine pulverized coal at 1400–1700 °C in coal fired power plants [5,6]. Bottom or fly ash is a good source of aluminosilicates which is being utilized not only because of its low cost but also due to strict environmental regulations implemented by the governments [7]. Moreover, various kinds of foamy ceramic construction materials (materials used for thermal insulation of the buildings like foamed cement insulation boards) are being preferred as the energy crises all over the world are becoming a big issue because of increasing demand and shortage of supply of energy. These foamy ceramic material are non load bearing part of the building to facilitate the conditioning of inside environment. There are different ways of converting ceramic mortars into

* Corresponding author.
E-mail addresses: amonehsan@uet.edu.pk, amonehsan@hotmail.com (E.U. Haq).

http://dx.doi.org/10.1016/j.conbuildmat.2016.08.135
0950-0618/

Table 1
Sample IDs and their respective compositions.

Sample ID	Bottom ash (%)	Sodium silicate (%)	Sodium hydroxide (%)	Expansion by irradiation (%)
BGF0	50	50	0	206
BGF1	50	49	1	98.2
BGF3	50	47	3	86.5
BGF5	50	45	5	80.1
BGF7	50	43	7	76.1

foams like by using some gas releasing agents while mixing and grinding and which produce internal voids and convert the mortar or slurry to foams. These gas releasing agents can either be inorganic or organic in nature [1]. Sodium silicate is one the foaming agents effectively utilized in production of fly ash based ceramic foams which are produced around 900 °C using sodium borate as a fluxing agent [8]. Microwaves are the source of energy, where the deep penetration of thermal agitations can be produced without touching the mass and now a days are especially being utilized in handling and controlling the hazardous materials [9–12]. In this paper the effect of alkali over the processing of the bottom ash based foam enhanced by microwave irradiation has been discussed. Samples with different percentage of alkali (sodium hydroxide) were produced using different amounts of sodium silicate and bottom ash. Whereby, the samples without alkali activation were produced just in absence of alkali additions. Then thermal agitation was provided by the microwave radiation.

2. Experimental program

2.1. Materials and processing

The bottom ash was obtained from ENEL coal fired power station near Brindisi Italy. Water glass with 9% Na_2O, 30% SiO_2 and 61% H_2O and specific gravity of 1.35 g/cm^3, was utilized in the experimentation as a foaming agent. Sodium hydroxide (Cloverinvest/Italy) was utilized as an activation agent in the case of alkali activated categories. The 14 M alkali solution was added in different percentages as shown in Table 1 [2,13]. Two different categories with and without alkali activation, slurries with different proportions of the bottom ash and sodium silicate, were produced. The slurry was prepared in planetary ball mill with alumina balls as grinding media for 10 min. The liquid slurry was poured to Teflon cylindrical vessels and irradiated in (EM 45 mls 1200 mega MILESTONE) at power of 900 W for 4 min in two steps; two minutes in the Teflon mold and 2 min after demolding. The first two minutes to make the slurry foam and the later to dehydrate and dehydroxilate the foam, making it insoluble to water. The samples

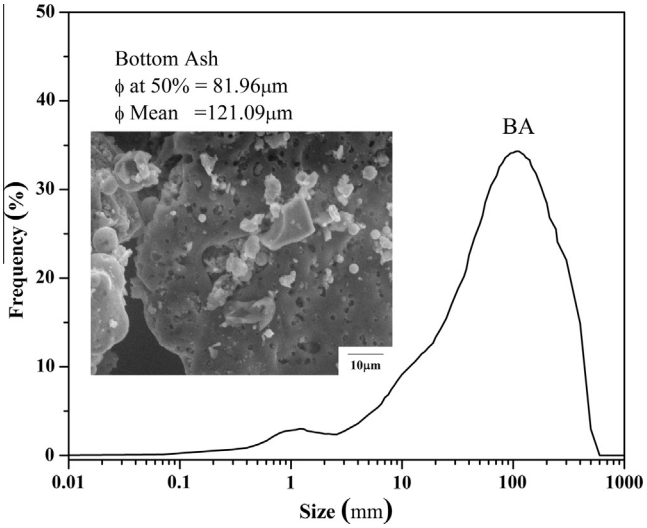

Fig. 1. Particle size distribution and SEM micrograph of bottom ash.

were cut with hacksaw and lapped to make fit for the various tests for characterizations.

2.2. Characterization of samples

Chemical composition of bottom ash was measured by X-ray fluorescence spectrometer (Bruker M4 Tornado). Major part of bottom ash was composed of silica 52%, alumina 22%, Fe_2O_3 17% and CaO 6%. The particle size distribution was evaluated by particle size analyser (Cilas 1190) and the mean diameter found to be 121 μm. ATR (Attenuated Total Reflectance; Perkin Elmer) was used to evaluate the FTIR spectra of ash and samples with a diamond crystal as a probe. Micrographs were generated by scanning electron microscope (Model: Zeiss, Jena, Germany) to analyse the pore structure and pores morphology.

The apparent and bulk densities were calculated by Quantachrome density analyser for the former and mass volume ratio for the latter case. The percentage porosity was measured by the following relationship.

$$\% \text{ Porosity} = 1 - \rho/\rho_a$$

where ρ, ρ_a are bulk and apparent densities respectively [14].

Thermal conductivities of different samples were measured using TCi thermal analyser (SETARAM) which is transient plane technique. The mechanical properties of the foams were measured by Lloyd LR5K compression testing machine using standard protocol of ASTM C109.

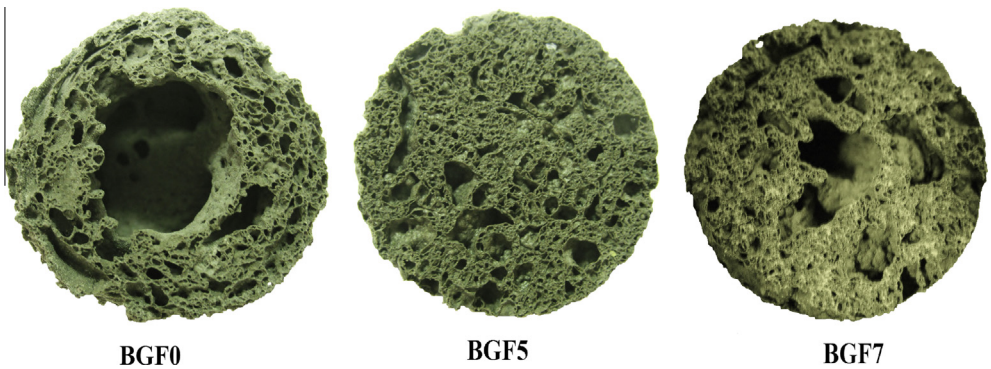

Fig. 2. Piping in the processed sample of BGF0 and uniform BGF5 samples.

3. Results and discussion

3.1. Effect of alkali on foamability

As alkali was added to the ashes, the foamability of samples was decreased as in case of BGF5 the slurry swelled upto 83.3% while in other case BGF0 it was upto 156.5%; almost double of the former case. This was due to the collapse of the structure of the individual bottom ash particles due to dissolution in alkali solution. The intumescence of other compositions are given in the Table 1. The bottom ash particles structure composed of fine pores which were filled with water during its cooling at power plant; visible also in the SEM micrograph of bottom ash as shown in Fig. 1. The microwaves penetrate deep down the middle of the samples, create thermal agitations and hence convert the water to steam [15]. The foaming was mainly because of sodium silicate where water created steam and swelled the mass to a porous scaffold. It was further observed that by similar process, it was difficult to produce foam by fly ash where particles were spherical and impermeable to water but for bottom ash it was produced successfully due to the fine inherent porosities. This process of steam creation and foaming of bottom ash mortar was similar to foaming of perlite (a naturally occurring amorphous volcanic glass which expands when heated upto 800 °C and that has a relatively high water content, typically formed by the hydration of obsidian) [16]. Because of absence of these porosities, fly ash slurries were difficult to foam compared to bottom ash slurries. Similarly, when bottom ash was alkali activated by the addition of sodium hydroxide, its increasing attack over the particles dissolved the micro porous structure partially to completely with increasing percentage of alkali addition. Hence bottom ash particles resulted in lesser volume expansion when their slurries were alkali activated.

3.2. Effect on pore morphology

The pore morphology of the samples without alkali activation showed a big hollow pipe in the center of the samples as shown in the Fig. 2 (BGF0) where bottom ash was not activated. The reason behind this pipe was the accumulation of low density and highly porous mass containing highest amount of water over the surface. This higher amount of water produced very high pressure steam creating a big void at the upper surface under the thin domed layer of uniform mass. There was no big void or pipe observed in the BGF samples until 5% of alkali activation and the porosity was distributed uniformly compared to BGF0. This pipe again appeared at BGF7 but inside a dense less porous foam. The SEM micrographs were produced to compare the pore morphologies of the two categories as shown in the Fig. 3. Fig. 3a is a micrograph of BGF0 at lower magnification, indicating the micropores shapes from bigger irregular to small spheroidal. The network itself contains very fine porosity whose detail is clear in Fig. 3b at relatively higher magnification. The continuous network indicates the fine pores which are not produced during foaming but are inherited from the bottom ash particles. Fig. 3c is the micrograph of BGF5 where the pores are uniform and much less irregular compared to former case. The network or walls of the pores are less porous compared to BGF0 due to dissolution and regeneration of the porosity during microwave foaming. The finer detail of the walls or network is given in Fig. 3d. Although there are very fine pores still present but compared to BGF0 (Fig. 3b) these are very few and smaller in size.

3.3. Effect on pore size distribution

Bimodal pore size distribution was observed in the BGF0 samples as shown in Fig. 4. The finer pores were inherent from the bottom ash particles because there was no activating or dissolving solution but just the mechanical attrition forces during milling. The wide pore size distribution was because of irregularities in the bottom ash particles which produced different levels of steam pressures and created the pores in vicinity of particles. The micropores in the range of 0.04–0.1 μm are the same pores visible in SEM micrograph but these pores are not present in BGF5 because of the attack of alkali; dissolution of the particles hence removing the inherent pores. Here in BGF5, the pore size range is

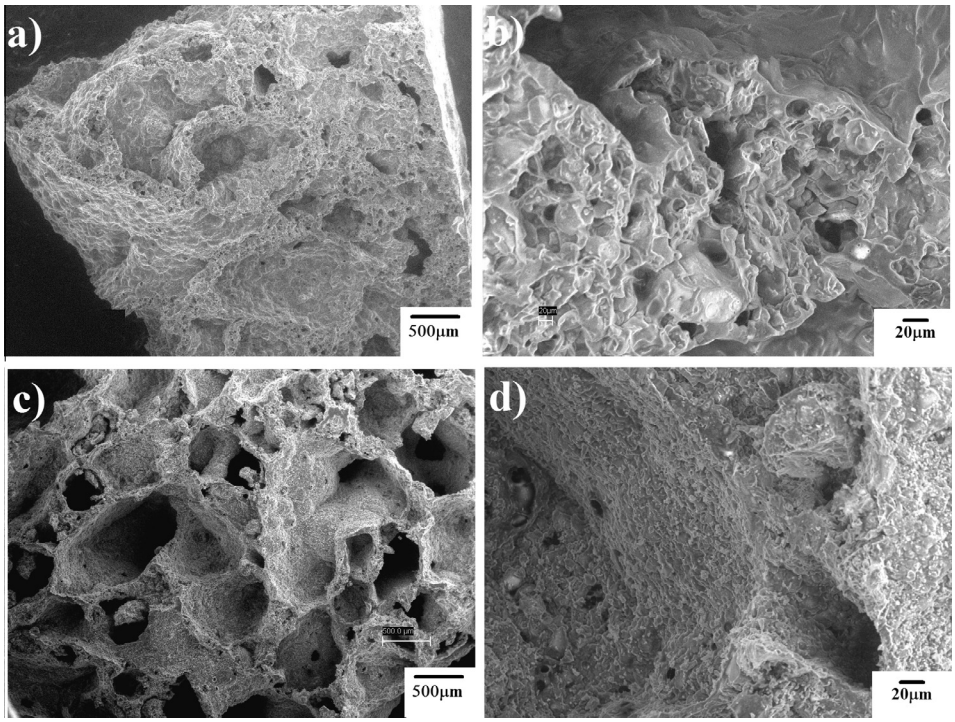

Fig. 3. SEM micrographs of BGF0 (a, b) and BGF5 (c, d) at lower (100×) and higher (1000×) magnifications.

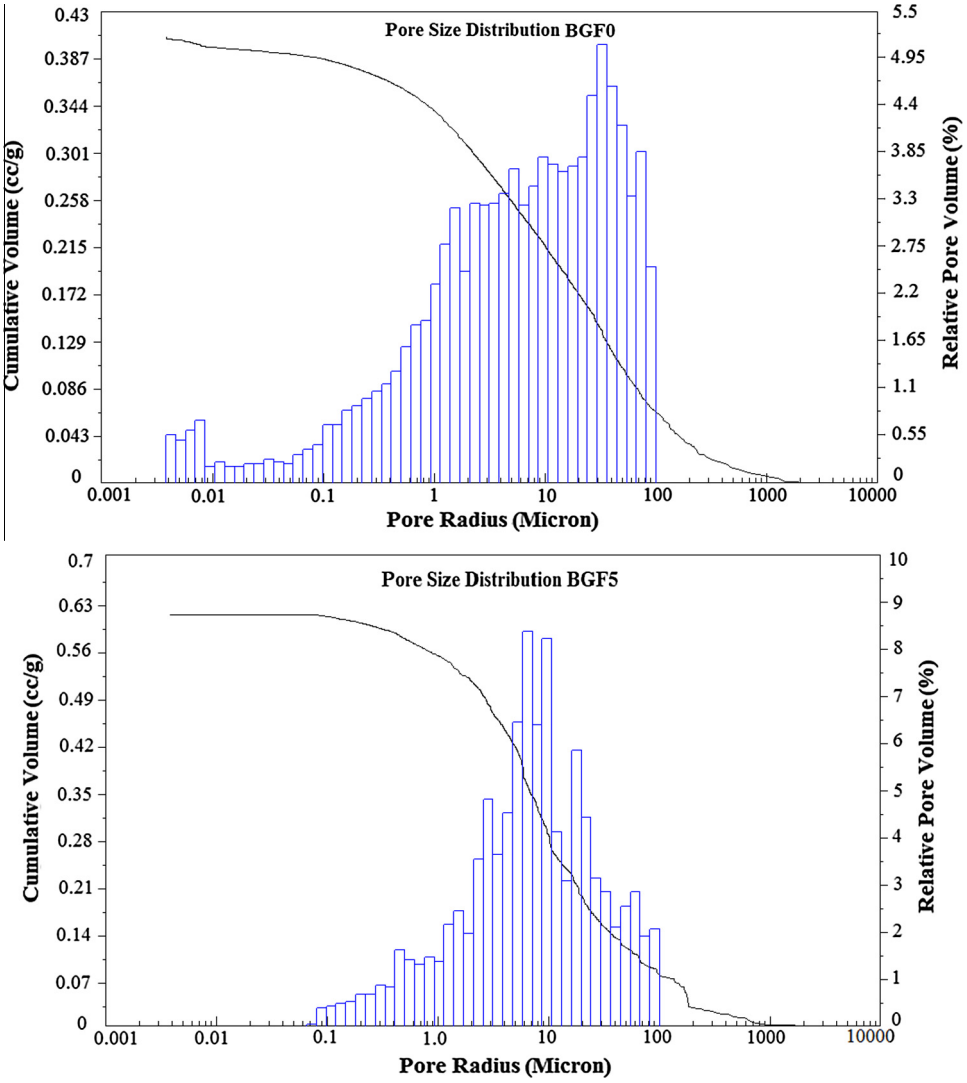

Fig. 4. Pore size distribution of BGF0 and BGF5 by Mercury Porosimetry.

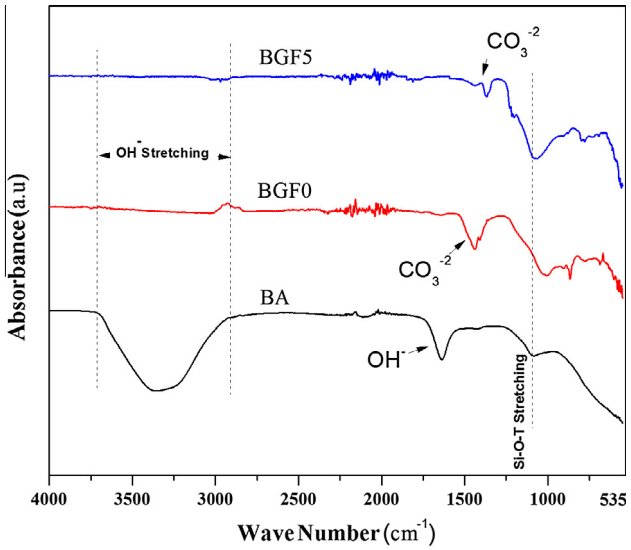

Fig. 5. FTIR spectra of bottom ash (BA), BGF0 and BGF5.

0.1–100 μm which is less compared to BGF0 (from 0.004 to 100 μm). The average pore size for the BGF0 is 32 while for the BGF5 is 6 μm.

3.4. Effect on molecular vibrations

The molecular bending and stretching behaviour provide much information about the types of bonding between the molecules and atoms during geopolymerization reaction and this behaviour can be studied through FTIR technique. The FTIR spectra of the bottom ash (BA), BGF0 and BGF5 are given and compared in the Fig. 5. The stretching vibrations for Si-O-T(T:Si or Al) for bottom ash indicate two things, i) there is no geopolymerization reaction and ii) Al is still present in octahedral position being higher in wave number 1086 cm^{-1}. This higher wavenumber is lowered as soon as the long chain molecules of geopolymers are formed [13,17]. The same vibrations for the BGF0 are little bit moved towards lower wave number 1060 cm^{-1}, indicating the small amount of geopolymerization reaction due to a small activation because of presence of alkali in the sodium silicate solution. But the difference between BA and BGF0 is not too much attributed to smaller amounts of sodium hydroxide hence lesser dissolution which is also indicated by SEM micrographs. On the other hand for BGF5, this vibration band is lowered

Table 2
Various properties of the foamed samples.

Sample ID	Density (g/cm^3)	Apparent density (g/cm^3)	Thermal cond. (W/m K)	Mech. strength (MPa)	Young's modulus (GPa)	Porosity (%)	Average pore radius (μm)	Surface area (m^2/g)
BGF0	0.50	2.08	0.074	1.2	0.045	75.9	32.56	4.25
BGF1	0.52	2.06	0.09	2.1	0.08	74.7	11.21	1.5
BGF3	0.54	2.02	0.087	2.4	0.088	73.26	9.74	0.81
BGF5	0.64	2.01	0.081	3.15	0.127	68.1	6.37	0.58
BGF7	0.69	2.0	0.080	3.45	0.15	65.5	4.24	0.56

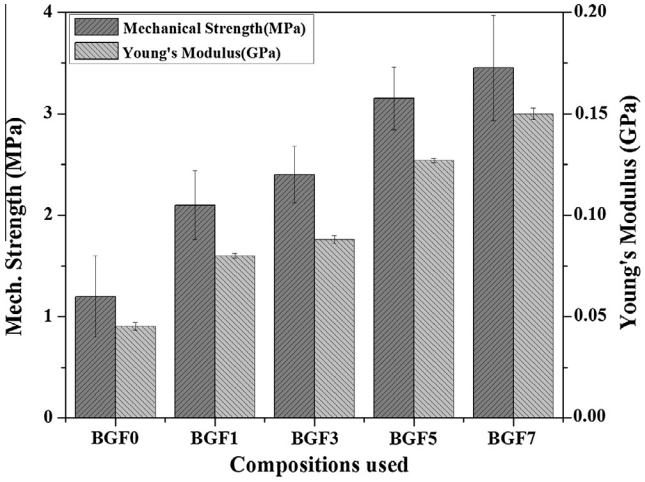

Fig. 6. Mechanical strength and Young's moduli comparison of different BGF's.

significantly upto 1000 cm^{-1}, compared to BA and BGF0, due to higher dissolutions of bottom ash particles and also higher level of geopolymerization achieved ever before for geopolymer foams [18]. In doing this, in fact, the Al is transferred from octahedral to tetrahedral position which is an indication of geopolymerization reaction [13,19]. The OH^- stretching vibrations are highest in the bottom ash being a host to water while these vibrations are decreased in BGF5 and BGF0. In BGF5, these vibrations are bit higher than BGF0 due to small average pore size thus higher capillary forces to retain water inside. The other CO_3^{-2} vibrations are due to presence of sodium carbonate where CO_2 is absorbed in sodium silicate solution during handling and mixing from the atmosphere. These vibrations are lesser in BGF0 due to lesser amount of sodium hydroxide present in the slurry; from sodium silicate [20].

3.5. Density, porosity and thermal conductivity

The effect of alkali over the density and thermal conductivity was much pronounced, not only physically observable but also can be deduced from the previous discussion as shown in the Table 2. The thermal conductivity was increased as the sodium silicate amount was increased during preparation of geopolymer foam. The apparent density of the BGF0 was measured to be higher due to higher porosity and at the same time bulk density was decreasing from BGF1 to BGF7. The thermal conductivity also increased as the alkali was added more and more due to formation of denser structure hence increasing the bulk density. The density obtained was much lower than other conventional geopolymer foam processing methods. Also the thermal conductivity was in similar range to other geopolymer foams [21,22].

3.6. Mechanical strength

Mechanical strength of the foamed samples increased by the level of activation due to formation of finer pores and lower surface area hence higher bulk densities. The highest mechanical strength was achieved for BGF5 and BGF7 but as discussed earlier that BGF7 was prone to piping similarly like BGF0 so wasn't considered as optimum composition. Strength was greatly improved by the addition of alkali in the geopolymer foam processing i.e. BGF5 had almost double strength compared to BGF0. This happened due to pores refinement, reduction in overall porosity, narrow pore size distribution and higher degree of geopolymerization as indicated in FTIR investigation. The irregular pore morphology was also a reason for exhibition of lower mechanical properties by BGF0 because the big voids were the point of stress concentration during mechanical loading leading to crack initiation and propagation. The particles joined edge to edge or surface to surface in BGF0 were even point of weakness being themselves porous (bimodal porosity) in nature. So these particles cannot be compared in strength to those uniforms and with regular unimodal porous mass as in the case of BGF5. The particles in BGF5 had uniform morphology as well compared to BGF0. Similarly the higher and higher Young's modulus was observed from BGF0 to BGF7 samples as sown in Fig. 6. The measured mechanical strength for different compositions is higher than commercially available geopolymer foams like TROLIT™ [15].

4. Conclusion

This research studies the effects of the alkali activation over foamability, physical and mechanical properties of the bottom ash foam. By addition of alkali, the porosity can be tailored according to required shape and amount although the foamability is reduced almost half way around for the optimum composition. Both methods (with and without alkali activation) seem valuable in their own perspectives and their adoption may be regarded as applications specific. But as a successful construction material, the better mechanical properties are achieved if before foaming, the bottom ash is activated by the addition of alkali. BGF0 production method is advantageous where the material is required with higher specific surface area etc. Alkali activates the mass by the dissolution of the particles of bottom ash and later during polycondensation the structure regenerates and long chain geopolymers are formed which ultimately enhance the strength of the foam as indicated in FTIR analysis. Although alkali activates the bottom ash particles but still the morphologically irregular particles contain water which produced enough steam during foaming to be resulted in the foamed mass. The BGF5 production method is suitable in producing the thermal isolating bricks and block as uniform porosity is created throughout the mass.

References

[1] Z. Zhang, J.L. Provis, A. Reid, H. Wang, Geopolymer foam concrete: an emerging material for sustainable construction, Constr. Build. Mater. 56 (2014) 113–127.
[2] J. Temuujin, A. van Riessen, K.J.D. MacKenzie, Preparation and characterisation of fly ash based geopolymer mortars, Constr. Build. Mater. 24 (2010) 1906–1910.
[3] B. Nematollahi, J. Sanjayan, Effect of different superplasticizers and activator combinations on workability and strength of fly ash based geopolymer, Mater. Des. 57 (2014) 667–672.

[4] G. Görhan, G. Kürklü, The influence of the NaOH solution on the properties of the fly ash-based geopolymer mortar cured at different temperatures, Compos. Part B 58 (2014) 371–377.
[5] S.M. Nyale, O.O. Babajide, G.D. Birch, N. Böke, L.F. Petrik, Synthesis and characterization of coal fly ash-based foamed geopolymer, Procedia Environ. Sci. 18 (2013) 722–730.
[6] M. Ahmaruzzaman, A review on the utilization of fly ash, Prog. Energy Combust. Sci. 36 (2010) 327–363.
[7] M. Erol, S. Kucukbayrak, A. Ersoy-Mericboyu, Characterization of coal fly ash for possible utilization in glass production, Fuel 86 (2007) 706–714.
[8] X. Chen, A. Lun, G. Qu, Preparation and characterization of foam ceramics from red mud and fly ash using sodium silicate as foaming agent, Ceram. Int. 39 (2013) 1923–1929.
[9] K. Somna, C. Jaturapitakkul, P. Kajitvichyanukul, P. Chindaprasirt, NaOH-activated ground fly ash geopolymer cured at ambient temperature, Fuel 90 (2011) 2118–2124.
[10] S. Jumrat, B. Chatveera, P. Rattanadecho, Dielectric properties and temperature profile of fly ash-based geopolymer mortar, Int. Commun. Heat Mass Transfer 38 (2011) 242–248.
[11] J. Somaratna, D. Ravikumar, N. Neithalath, Response of alkali activated fly ash mortars to microwave curing, Cem. Concr. Res. 40 (2010) 1688–1696.
[12] E.U. Haq, S.K. Padmanabhan, A. Licciulli, Microwave synthesis of thermal insulating foams from coal derived bottom ash, Fuel Process. Technol. 130 (2015) 263–267.
[13] W.K.W. Lee, J.S.J. van Deventer, Use of infrared spectroscopy to study geopolymerization of heterogeneous amorphous aluminosilicates, Langmuir 19 (2003) 8726–8734.
[14] K.P. Sanosh, E.U. Haq, A. Licciulli, Synthesis of silica cryogel-glass fiber blanket by vacuum drying, Ceram. Int. 42 (2016) 7216–7222.
[15] M. Lach, K. Korniejenko, J. Mikula, Thermal insulation and thermally resistant materials made of geopolymer foams, Procedia Eng. 151 (2016) 410–416.
[16] P. Chindaprasirt, C. Jaturapitakkul, W. Chalee, U. Rattanasak, Comparative study on the characteristics of fly ash and bottom ash geopolymers, Waste Manage. 29 (2009) 539–543.
[17] S.M. Nyale, O.O. Babajide, G.D. Birch, N. Böke, L.F. Petrik, Synthesis and characterization of coal fly ash-based foamed geopolymer, Procedia Environ. Sci. 18 (2013) 722–730.
[18] V.F.F. Barbosa, K.J.D. MacKenzie, C. Thaumaturgo, Synthesis and characterisation of materials based on inorganic polymers of alumina and silica: sodium polysialate polymers, Int. J. Inorg. Mater. 2 (2000) 309–317.
[19] E.U. Haq, S.K. Padmanabhan, A. Licciulli, Synthesis and characteristics of fly ash and bottom ash based geopolymers – a comparative study, Ceram. Int. 40 (2014) 2965–2971.
[20] H. Xu, Q. Li, L. Shen, W. Wang, J. Zhai, Synthesis of thermostable geopolymer from circulating fluidized bed combustion (CFBC) bottom ashes, J. Hazard. Mater. 175 (2010) 198–204.
[21] V. Ducman, L. Korat, Characterization of geopolymer fly-ash based foams obtained with the addition of Al powder or H_2O_2 as foaming agents, Mater. Charact. 113 (2016) 207–213.
[22] P. Posi, C. Ridtirud, C. Ekvong, D. Chammanee, K. Janthowong, P. Chindaprasirt, Properties of lightweight high calcium fly ash geopolymer concretes containing recycled packaging foam, Constr. Build. Mater. 94 (2015) 408–413.